Cluster production within antisymmetrized molecular dynamics

Akira Ono[1,a]

[1] *Department of Physics, Tohoku University, Sendai 980-8578, Japan*

Abstract. Clusters are quite important at various situations in heavy-ion collisions. Antisymmetrized molecular dynamics was improved to take into account the correlations to form light clusters, such as deuterons and α particles, and light nuclei composed of several clusters. The momentum fluctuations of emitted particles are also taken into account by a simple method. Formation of fragments and light clusters in a wide range of heavy-ion collisions was well described with a single set of model parameters. Fragmentation in a proton induced reaction was also well reproduced by introducing cluster correlations. Calculated results demonstrate strong impacts of clusters in various observables including those usually regarded as probes of the density dependence of symmetry energy.

1 Introduction

Fragments and light clusters are copiously produced in various kinds of nuclear reactions such as in heavy-ion collisions. For example, in Xe + Sn central collisions at 50 MeV/nucleon, the INDRA data [1] show that only 10% of total protons in the system are emitted as free protons and all the other protons are bound in light clusters and fragments in the final state. About 20% of protons are bound in α particles, about 10% are bound in clusters of $A = 2$ and 3, and about 60% are bound in heavier fragment nuclei. Even though the incident energy is raised, to 250 MeV/nucleon for example, the free-proton ratio is still about 20% as shown by the FOPI data [2] for the central Au + Au collisions. In these heavy-ion collisions, the system is first compressed and then expands relatively rapidly. The formation of fragments and light clusters should be closely related to the property of such expanding nuclear matter. On the other hand, the target nucleus can also break up into fragments in light-ion induced reactions, as in the experiments [3], even though the excitation of the nucleus does not primarily induce strong collective expansion. Formation of fragments and clusters is one of the essential features of these reactions, since they are produced in most of the events in these reactions with the participation of most of the nucleons in the system.

It has been a longstanding problem to understand fragment formation from microscopic points of view. Transport theories, which solve the time evolution of the many-nucleon system or its one-body distribution, have generally been a powerful approach to understand important aspects of collision dynamics in the Fermi energy domain and in higher energies. Among transport models, the molecular dynamics models [4–7] may be expected to be suitable for fragmentation reactions because many-nucleon correlations are handled at least in the sense of classical dynamics. However, studies have

[a] e-mail: ono@nucl.phys.tohoku.ac.jp

shown that some quantum features are required in order to properly describe fragment formation. The antisymmetrized molecular dynamics (AMD) approach [5] takes into account the full antisymmetrization of many-nucleon wave function, which is certainly an important quantum feature. Emergence of many fragmentation channels is also a crucial idea to consistently understand the fragment formation and the single-particle dynamics [8, 9]. Furthermore, light clusters are highly quantum objects because they have only one (or a few) bound state.

When light clusters are produced in reactions, they are probably still surrounded by other particles. The property of a cluster in idealistic nuclear medium is typically calculated with an inmedium Schrödinger equation as in the calculation by Röpke [11]. The effect of Pauli blocking is taken into account. A cluster can exist as a bound state, depending on the density of the medium and the momentum of the cluster relative to the medium. Then, in actual systems, many clusters may coexist and change the nuclear matter properties and the collision dynamics. During the time evolution, clusters will be repeatedly created and broken by reactions such as $p+n+X \leftrightarrow d+X'$, $p+n+d+X \leftrightarrow \alpha+X'$ and many others.

Recently the heavy-ion data from Texas A&M have been analyzed to extract the cluster composition and other properties of nuclear matter as functions of the evolution of the temperature and the density [12]. Comparison of the extracted equilibrium constants for the cluster composition with various equation-of-state (EOS) models suggests necessity of a cluster suppression mechanism such as medium effects [13]. Nevertheless, in general, the link between heavy-ion collisions and EOS should be carefully checked because of the dynamical nature of collisions.

It is therefore demanded that the transport models should solve the time evolution of collisions by correctly treating cluster correlations. However, transport models have been developed based on the single-nucleon motions, and only few models treat cluster correlations explicitly. In a version of BUU by Danielewicz *et al.* [14], clusters up to ^{3}H and ^{3}He have been introduced as new particle species and the equations for the distribution functions are coupled by the collision terms representing various reactions of clusters and nucleons. A recent calculation by this model demonstrates that collision dynamics is influenced by the clusters [15]. On the other hand, in the antisymmetrized molecular dynamics (AMD) approach, we have introduced cluster correlations by improving the two-nucleon collision procedure [16–18]. The aims of this article are to report the present status of this approach and to demonstrate the importance of clusters in the studies of heavy-ion collisions.

2 AMD approach

AMD uses a single Slater determinant of Gaussian wave packets [5],

$$\langle \mathbf{r}_1 \cdots \mathbf{r}_A | \Phi(Z) \rangle = \det_{ij} \Big[\varphi_{\mathbf{Z}_i}(\mathbf{r}_j) \chi_{\alpha_i}(j) \Big], \tag{1}$$

where the spatial wave functions of nucleons are given by

$$\langle \mathbf{r} | \varphi_{\mathbf{Z}} \rangle = \left(\frac{2\nu}{\pi} \right)^{3/4} \exp\Big\{ -\nu \Big(\mathbf{r} - \frac{\mathbf{Z}}{\sqrt{\nu}} \Big)^2 + \frac{1}{2} \mathbf{Z}^2 \Big\} \tag{2}$$

and χ_α is the spin-isospin wave function with $\chi_\alpha = p\uparrow, p\downarrow, n\uparrow$, or $n\downarrow$. Thus the many-body state $|\Phi(Z)\rangle$ is parametrized by a set of complex variables $Z \equiv \{\mathbf{Z}_i;\ i = 1, \ldots, A\}$, where A is the number of nucleons in the system. The width parameter $\nu = (2.5\ \mathrm{fm})^{-2}$ is treated as a constant parameter common to all the wave packets. The Gaussian wave packet $|\varphi_{\mathbf{Z}}\rangle$ has the minimum uncertainty $\Delta x \Delta p = \frac{1}{2}\hbar$ with $\Delta x^2 = 1/(4\nu)$ and $\Delta p^2 = \hbar^2 \nu$.

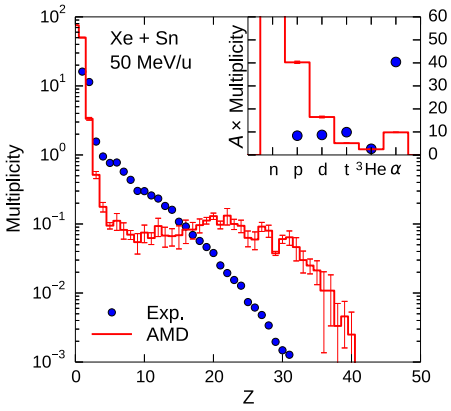

Figure 1. A result of AMD without cluster correlations (red historgram) for the fragment charge distribution in central Xe + Sn collisions at 50 MeV/nucleon. The INDRA data [1] are shown by blue points. The inset shows the number of nucleons in light particles.

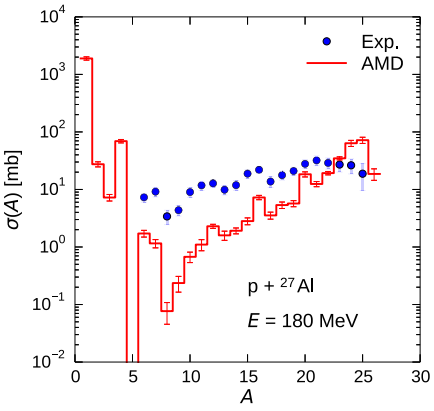

Figure 2. A result of AMD without cluster correlations (red histogram) for the fragment production cross sections in p + Sn collisions at 180 MeV. The experimental data [3] are shown by blue points.

The time evolution of the wave-packet centroids is determined by the motion in the mean field, derived from the time-dependent variational principle, and the stochastic two-nucleon collision process. The former is written as

$$i\hbar \sum_{j\tau} C_{i\sigma,j\tau} \frac{dZ_{j\tau}}{dt} = \frac{\partial \mathcal{H}}{\partial Z^*_{i\sigma}}, \qquad \mathcal{H}(Z) = \frac{\langle \Phi(Z)|H|\Phi(Z)\rangle}{\langle \Phi(Z)|\Phi(Z)\rangle} - \frac{3\hbar^2\nu}{2M}A + T_0(A - N_{\rm F}(Z)) \tag{3}$$

with a hermitian matrix $C_{i\sigma,j\tau}$ and the expectation value $\mathcal{H}$ of the effective Hamiltonian, such as the Skyrme interaction, with subtraction of spurious kinetic energies of fragments [5]. During the time evolution, any pair of two nucleons will collide with a suitable probability when the distance between them is small. A two-nucleon collision is treated as a quantum mechanical transition from an AMD state $|\Phi_i\rangle$ to another AMD state $|\Phi_f\rangle$ specified by a relative momentum between the scattered two nucleons $(p_{\rm rel}, \Omega)$. The transition rate is expressed as

$$v d\sigma = \frac{2\pi}{\hbar} |\langle \Phi_f|V|\Phi_i\rangle|^2 \delta(E_f - E_i) \frac{p^2_{\rm rel} dp_{\rm rel} d\Omega}{(2\pi\hbar)^3}, \tag{4}$$

assuming a unit normalization volume. In general, medium modification is introduced for the scattering matrix elements. It should be noted that some medium effect still exists also in the $p_{\rm rel}$-dependence of the final state energy E_f. The Pauli blocking for the scattered nucleons is taken into account [5].

2.1 AMD without clusters

In the usual treatment of two-nucleon collisions, only the states of the scattered two nucleons are changed in the final state $|\Phi_f\rangle$. See Ref. [5] for the precise description of the method which employs 'physical coordinates'.

It has been known for a long time that this very basic version of AMD does not well reproduce the fragmentation in collisions of heavy nuclei. For example, in Xe + Sn central collisions at 50 MeV/nucleon (see Fig. 1), the relatively heavy nuclei are produced too frequently and the yield of lighter intermediate mass fragments is too small. The production of α particles is seriously underestimated and nucleons are overproduced. The result after calculating the statistical decay of primary fragments is shown as well as in all the other figures in this article. A similar problem was observed in the Ca + Ca collisions at 35 MeV/nucleon [19]. The basic version of AMD was applied to the fragmentation in the $p + {}^{27}$Al reaction at 180 MeV [20], where the breakup of the target nucleus does not happen sufficiently to reproduce the yield of light fragments. A similar result is shown in Fig. 2 calculated with a new code by turning off extensions. These problems cannot be solved by adjusting the effective interaction or the inmedium nucleon-nucleon cross sections.

In many cases, the reproduction of fragment yield was improved very much by introducing wave-packet splitting as a quantum branching process based on the single-particle motions with decoherence [8, 9, 19, 21]. However, a consistent reproduction of the yields of light clusters and light intermediate mass fragments has not been achieved by a single set of model parameters for all the reaction systems. This may suggest that the correlations to produce light clusters should be treated more explicitly.

It should be noted that the AMD wave function is suitable for describing cluster correlations in the ground state and low-lying excited states of nuclei [9]. When a cluster is placed in a nucleus within AMD, a reasonable value of the cluster-binding energy is obtained depending on the location and the center-of-mass momentum of the cluster [10]. The important question is, however, whether such clusterized states are realized with correct probabilities during the evolution of reactions. In fact, after a two-nucleon collision, one (or both) of the scattered nucleons may accidentally form a cluster with surrounding nucleon(s). The probability is governed by the classical phase space or the classical density of states $\tilde{D}(E)$ of the internal degrees of freedom of a cluster to be formed. The density of states is $\tilde{D}(E) = 0$ for $E < E_{\rm gs}$ below the ground state energy of the cluster, and it starts at $E = E_{\rm gs}$ continuously. Since the cluster-binding energy $|E_{\rm gs}|$ is small due to the cancellation of the potential and kinetic energies, the bound phase-space volume $\int_{E_{\rm gs}}^{0} \tilde{D}(E)dE$ cannot be large enough to correspond to a single quantum bound state. This is the reason why the cluster correlations do not emerge dynamically with reasonable probabilities. It is necessary to treat cluster correlations more explicitly as in the next subsection.

2.2 AMD with clusters

Light clusters have only one (or a few) bound state so that the density of states of the internal degrees of freedom is $D(E) = \delta(E - E_{\rm gs}) + D_{\rm continuum}(E)$. As mentioned above, the contribution of the discrete bound state cannot be suitably taken into account by the classical phase space of the wave packet centroids. To overcome this problem, an extension has been introduced [16] to allow direct formation of light clusters with $A = 2, 3$ and 4 in the final state $|\Phi_f\rangle$ in Eq. (4) for each two-nucleon collision. Namely, in this new method with cluster correlations, when two nucleons N_1 and N_2 collide, we consider the process

$$N_1 + N_2 + B_1 + B_2 \to C_1 + C_2 \tag{5}$$

in which each of the scattered nucleons N_j ($j = 1, 2$) may form a cluster C_j with a spectator particle B_j. This process includes the collisions without cluster formation as the special case of $C_j = N_j$ with empty B_j. The transition rate of the cluster-forming process is given by Eq. (4) with the suitable choice of the final state $|\Phi_f\rangle$. When a cluster is formed, the corresponding wave packets are placed at the same phase-space point, i.e., the cluster internal state is represented by the harmonic-oscillator $(0s)^n$

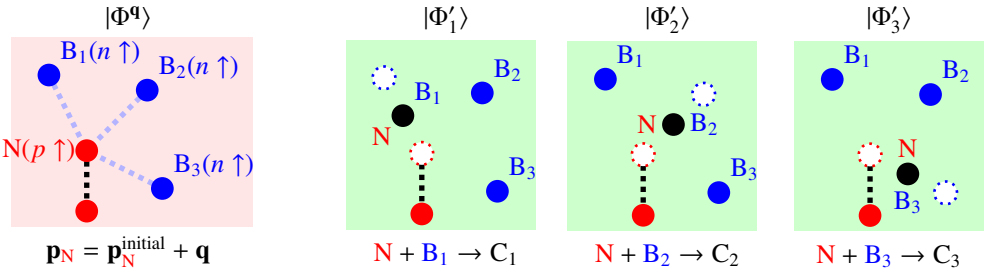

Figure 3. An example of deuteron formation in a two-nucleon collision, in which one of the scattered nucleon N (proton with up-spin) may form a deuteron cluster with any one of B_1, B_2 or B_3 (neutrons with up-spin). The filled circles depict the wave packet centroids. From Ref. [16].

configuration. Denoting the initial and final states of the $N_j + B_j$ system by $|\varphi_j\rangle$ and $|\varphi'_j\rangle$, respectively, we have the transition rate

$$v d\sigma = \frac{2\pi}{\hbar} |\langle\varphi'_1|\varphi_1^{\mathbf{q}}\rangle|^2 \, |\langle\varphi'_2|\varphi_2^{-\mathbf{q}}\rangle|^2 \, |M|^2 \, \delta(E_f - E_i) \frac{p_{\rm rel}^2 dp_{\rm rel} d\Omega}{(2\pi\hbar)^3}, \tag{6}$$

where $|\varphi_j^{\pm\mathbf{q}}\rangle = e^{\pm i\mathbf{q}\cdot\mathbf{r}_j}|\varphi_j\rangle$ are the states after the momentum transfer $\pm\mathbf{q}$ to the nucleons N_j ($j = 1, 2$), and $(p_{\rm rel}, \Omega)$ is the relative momentum between N_1 and N_2 in these states. The matrix element $|M|^2$ is the same as for the usual two-nucleon collisions. We use an average value of $|M|^2$ evaluated at $p_{\rm rel}$ and that evaluated at the initial relative momentum. The angular momentum conservation is taken into account by adjusting the collective rotation of the part near the colliding nucleons N_1 and N_2.

The actual situation of a two-nucleon collision requires more considerations because there are many possible ways of forming a cluster for each N of the scattered nucleons N_1 and N_2. For a scattered nucleon N, we first consider the possibility that N may form a cluster with one of the nucleons $\{B_k;\ k = 1, 2, \dots\}$ which have the same spin-isospin state (see Fig. 3). This spin-isospin state that is studied first is randomly decided. The cluster-formed state is denoted by $|\Phi'_k\rangle$ which is obtained, by first changing the state to $|\Phi^{\mathbf{q}}\rangle$ by the momentum transfer $\mathbf{q}$ to N, and then moving the two wave packets of N and B_k to the same phase-space point without changing their center of mass. Since the different final states are not orthogonal $\mathcal{N}_{kl} = \langle\Phi'_k|\Phi'_l\rangle \neq \delta_{kl}$, the probability that N forms a cluster with one of $\{B_k\}$ should be calculated as

$$P = \sum_{kl} \langle\Phi^{\mathbf{q}}|\Phi'_k\rangle \mathcal{N}_{kl}^{-1} \langle\Phi'_l|\Phi^{\mathbf{q}}\rangle = \sum_k |v_k|^2, \tag{7}$$

$$v_k = \sum_l \mathcal{N}_{kl}^{-1/2} \langle\Phi'_l|\Phi^{\mathbf{q}}\rangle, \tag{8}$$

This probability is calculated with an approximation that the many-body state is a direct product of wave packets centered at the 'physical coordinates' [5]. With the calculated probability P, a cluster will be formed with one of $\{B_k\}$. It is somewhat arbitrary which one of $\{B_k\}$ should be chosen with what probability. In the present calculations, we choose B_k with the relative weight $|v_k|^{2\gamma}$ with the parameter $\gamma = 2.0$. This partial probability should replace the overlap probability $|\langle\varphi'_1|\varphi_1^{\mathbf{q}}\rangle|^2$ or $|\langle\varphi'_2|\varphi_2^{-\mathbf{q}}\rangle|^2$ in Eq. (6). With the rest of the probability $(1-P)$, the particle N does not form a cluster with a nucleon of this spin-isospin state. The procedure is repeated for other spin-isospin states for B. The particle N in the above description should be regarded as a cluster, instead of a scattered nucleon, if a (sub)cluster has been already formed in previous steps of the repetition. Thus the formation of light clusters is

considered up to an α particle. It should be noted that the probability factors for different combinations of the formed clusters (C_1, C_2) decided in this way are functions of $p_{\rm rel}$ (or the momentum transfer $\mathbf{q}$) and the value of $p_{\rm rel}$ that conserves the energy depends on (C_1, C_2). A numerical procedure has been developed to treat this situation consistently.

Even when the cluster formation is introduced, the many-body state is always represented by an AMD wave function which is a Slater determinant of nucleon wave packets. The time evolution of the many-body state is solved just as usual without depending on whether some of the wave packets form clusters due to collisions in the past (except for the cluster-cluster binding process and for the momentum fluctuation in the next subsections). This is in contrast to the case of a version of BUU by Danielewicz *et al.* [14] where clusters are treated as new particle species. In our approach, a cluster may be broken by the mean field or by a two-nucleon collision between a nucleon in it and another nucleon in the system like a process $d + X \to n + p + X'$. It is also possible that, in the final state of this two-nucleon collision, the same cluster is formed again like an elastic process $d + X \to d + X'$. Thus various kinds of cluster reactions are taken into account without introducing many parameters. We only need to assume some inmedium two-nucleon cross sections (or matrix elements). In the calculations in the next section, we have chosen a so-called screened cross section [15]

$$\sigma_{\rm NN} = \sigma_0 \tanh(\sigma_{\rm free}/\sigma_0), \quad \sigma_0 = y\rho^{-2/3}, \quad y = 0.85. \tag{9}$$

In our previous works [10, 16, 17], it was necessary to introduce a reduction factor for the overall cluster-formation probabilities to reproduce multifragmentation data. In the present work, however, such a reduction factor does not seem necessary any longer when the momentum fluctuation is taken into account (see Sec. 2.4).

2.3 Cluster-cluster binding process

Many of light nuclei (Li, Be *etc.*) have only one or a few bound states which may be regarded as bound states of internal clusters. The quantum-mechanical probability of forming such a nucleus is not consistent with the semiclassical phase space with which it can be formed in the standard treatment of AMD. Therefore, for a better description, inter-cluster correlation is introduced as a stochastic process of binding clusters.

The basic idea is to replace the relative momentum between clusters by zero if moderately separated clusters ($1 < R_{\rm rel} < 7$ fm) are moving away from each other with a small relative kinetic energy ($\mathbf{R}_{\rm rel} \cdot \mathbf{V}_{\rm rel} > 0$ and $\frac{1}{2}\mu V_{\rm rel}^2 < 8$ MeV). In addition to these conditions, linking is allowed only if each of the two clusters is one of the three closest clusters of the other when the distance is measured by $[(\mathbf{R}_{\rm rel}/3\ {\rm fm})^2 + (\mathbf{V}_{\rm rel}/0.25c)^2]^{1/2}$, so that linking usually occurs in dilute environment. Non-clustered nucleons are treated here in the same way as clusters but two nucleons are not allowed to be linked. Two clusters also should not be linked if they can form an α or lighter cluster due to the combination of their spins and isospins. It is possible that more than two clusters are linked by this condition. However, only in the case that the mass number of the linked system is in the range $6 \le A_{\rm CC} \le 10$, the binding is performed for the linked system. The binding eliminates the velocities of clusters in the center-of-mass frame of the linked system. This combined system is called CC below.

The energy conservation should be achieved by scaling the relative radial momentum between a third particle and the center-of-mass of CC. The angular momentum is also conserved by adjusting the collective rotation of the part near CC. A reasonable way to choose a third particle may be to find a cluster which has participated in a collision that formed one of the clusters in CC. However, since we do not keep the full history of collisions in our computation, we choose a particle (a cluster or a

non-clustered nucleon) that has the minimal value of

$$\frac{(r + 7.5\ \mathrm{fm})(1.2 - \cos\theta)}{\min(\varepsilon_{\parallel},\ 5\ \mathrm{MeV})} \times \begin{cases} 1/2.7 & \text{if the particle is a non-clustered nucleon} \\ 1/2.1 & \text{if the particle is in an already combined system CC}' \\ 1 & \text{otherwize} \end{cases} \tag{10}$$

as the third particle for energy conservation, where r and $\varepsilon_{\parallel}$ are the distance and the radial component of the kinetic energy for the relative motion between the third particle and CC. The factor with the angle θ between the relative coordinate ($\mathbf{r}$) and velocity ($\mathbf{v}$) is introduced so as to favor the case of $\mathbf{r} \parallel \mathbf{v}$.

Clusters in already-formed combined systems are handled in some exceptional ways. If the third particle selected for the energy conservation belongs to a combined system (CC′) formed at a former time step, then CC′ is treated as the particle for the energy conservation and the internal velocities in CC′ are also eliminated to stabilize it. In the process to search CC, two clusters are not linked if they belong to different already-formed combined systems. If two clusters belongs to the same already-formed combined system, the condition $\mathbf{R}_{\mathrm{rel}} \cdot \mathbf{V}_{\mathrm{rel}} > 0$ is not required. Two-nucleon collisions are forbidden among nucleons within the same already-formed combined system, for a technical reason to keep the identity of the combined system.

2.4 Momentum fluctuation of emitted particles

The momentum fluctuation is also a longstanding problem in molecular dynamics approach for quantum systems. Due to the uncertainty principle, any single-particle state has a certain momentum width Δp as far as the particle is localized in coordinate space like a Gaussian wave packet. This is a reasonable description of nucleons in a nucleus. When a particle is emitted, however, it is reasonable to project the many-body state onto the states in each of which the emitted particle has a definite momentum. This idea has been introduced into AMD by the wave-packet splitting as a quantum branching process based on the single-particle motion with decoherence [8, 9, 19, 21]. However, this method treats only the independent motions of nucleons in the mean field.

In the present work with cluster correlations, we employ the simplest method proposed in Ref. [22] with a straightforward extension to clusters. A particle (a nucleon, a cluster or a combined system of clusters) is regarded as emitted if there is no other particle within the distance of 4 fm. When a particle is emitted, a momentum fluctuation is randomly given to it according to the momentum distribution of the wave packet $f(\mathbf{p}) \propto e^{-(\mathbf{p}-\mathbf{P})^2/2\Delta p^2}$ with $\Delta p^2 = A\hbar^2\nu$, where A is the mass number of the particle and ν is the width parameter of the nucleon wave packets. We search a part of the system that is likely a source which emitted the particle. The relative momentum between the particle and the emitting source is scaled for the consistency with the method of the subtraction of the spurious kinetic energies of fragments (see Ref. [22]). The center-of-mass momentum and the internal momenta of the emitting source are adjusted for the conservation of the total momentum and the total energy, respectively. The angular momentum is also conserved by adjusting the collective rotation of the emitting source.

The momentum fluctuation of emitted particles not only affects the spectra of those emitted particles, but also influences the stability of the rest of the system. Through the momentum and energy conservation, the fluctuation acts as pressure to reduce the expansion of the emitting source and/or it lowers the internal energy of the emitting source on average. Due to these effects, the two-nucleon collision process with clusters can be done without artificial adjustments, and the cluster-cluster binding process can be done with a relatively natural way, compared to the previous studies [10, 16, 17].

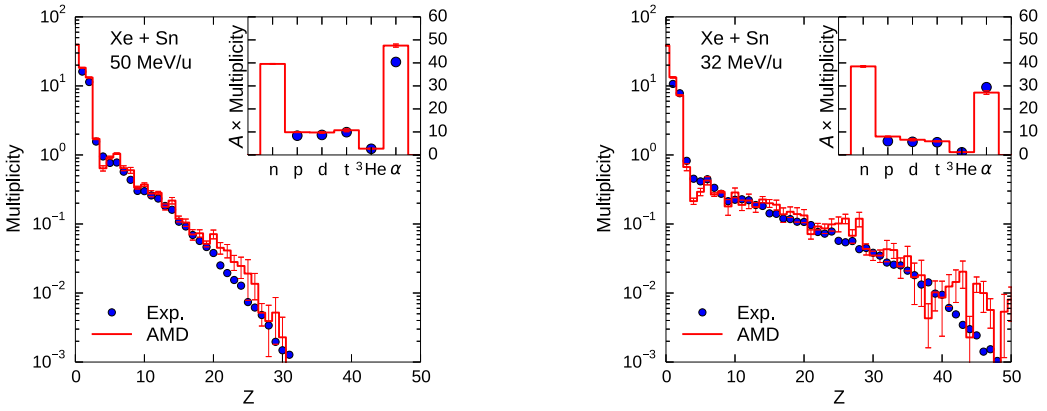

Figure 4. Fragment charge distribution in central Xe + Sn collisions ($0 < b < 2$ fm) at the incident energies of 50 (left) and 35 (right) MeV/nucleon, calculated by AMD with cluster correlations. The inset shows the multiplicities of light particles multiplied by the mass number. The INDRA experimental data are taken from Ref. [1].

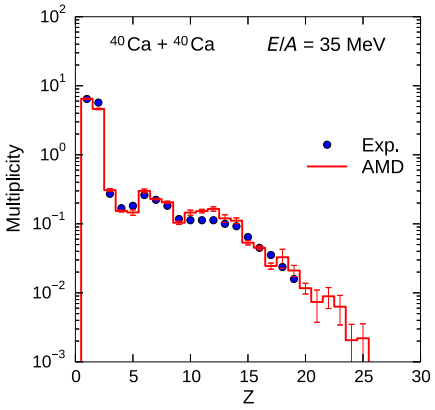

Figure 5. Fragment charge distribution in violent events in ^{40}Ca+^{40}Ca collisions at 35 MeV/nucleon. A filter for the experimental setup has been applied to the calculated events, and the violent events are selected by the same condition as for the experimental data [24].

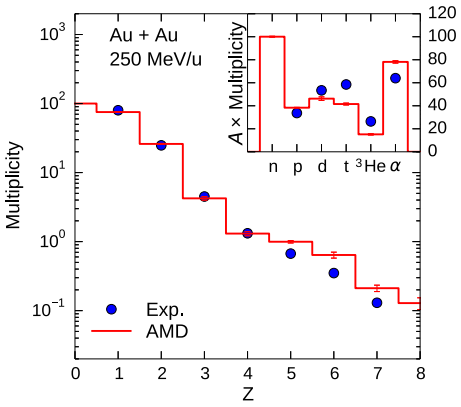

Figure 6. Fragment charge distribution in central Au + Au collisions at 250 MeV/nucleon. The calculated result by AMD with cluster correlations is compared to the FOPI experimental data [2].

3 Basic characters of multifragmentation

In this section, the calculated fragment charge distributions for multifragmentation in some central collisions are shown in comparison with experimental data. All the calculations were performed with the AMD with cluster correlations with the same model parameters as described in the previous section. The Skyrme SLy4 interaction was adopted with the spin-orbit term neglected. For high energy collisions at 250 MeV/nucleon, the momentum dependence of the Skyrme interaction was modified

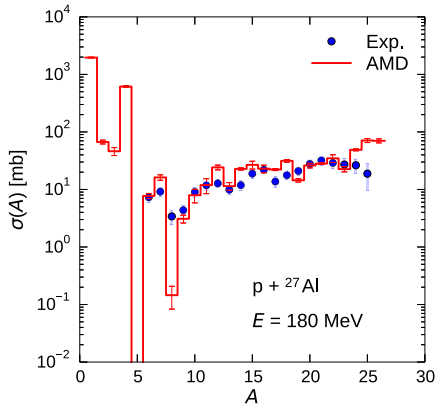

Figure 7. Fragment production cross sections in p + Sn collisions at 180 MeV calculated by AMD with cluster correlations. The experimental data [3] are shown by blue points.

in a similar way to Ref. [23] as described in Ref. [17]. The decays of excited fragments at the end of the AMD calculation were calculated by a statistical decay code.

Similar results were presented in Ref. [18]. The results here, however, have been updated with the improved framework as explained in the previous section.

Figure 4 shows the comparison for Xe + Sn collisions at 50 and 32 MeV/nucleon. The light particle multiplicities (multiplied by the particle mass number) are also shown in the inset. The overall distribution of the fragments ($Z \geq 3$) and the individual multiplicities of light charged particles are all reproduced very well. The deviations in the yields around $Z = 4$ at both energies have not been well understood. As well as the cluster correlations (to form clusters up to α particles), the cluster-cluster correlations are quite important to reproduce the data at both incident energies simultaneously.

The fragment multiplicities are calculated by the same model for violent collisions of ^{40}Ca + ^{40}Ca at 35 MeV/nucleon (Fig. 5) and central collisions of Au + Au at 250 MeV/nucleon (Fig. 6). The reproduction of data is almost satisfactory if we consider the wide difference of the system sizes and the incident energies. The α particles in Ca + Ca at 35 MeV/nucleon are underproduced in contrast to the overproduction in Xe + Sn at 50 MeV/nucleon. However, the reproductions of these two systems are much more consistent than with any other previous versions of AMD. The yield of relatively heavy fragments in the Au + Au collision may depend on the details of the cluster-cluster binding process.

Fragmentation in p + ^{27}Al at 180 MeV was also studied with cluster correlations. The result in Fig. 7 should be compared with Fig. 2 to find a strong influence of cluster correlations to produce medium mass fragments sufficiently. In the case with cluster correlations, we also find that the fragment yields for $A \lesssim 15$ is sensitive to the assumed inmedium two-nucleon cross sections. To reproduce the data, in the calculation for Fig. 7, it was necessary to choose a weaker reduction of cross sections in medium [$y = 4$ in Eq. (9)] and a weaker condition for Pauli blocking than in other calculations for heavy-ion collisions.

The yields of clusters and fragments in these various reaction systems represent the essential information on how many-body spatial correlations develop in expanding systems with various expansion speeds and/or thermal excitations. A consistent description of this feature is an important milestone to enable precise studies of other features, as in the following section.

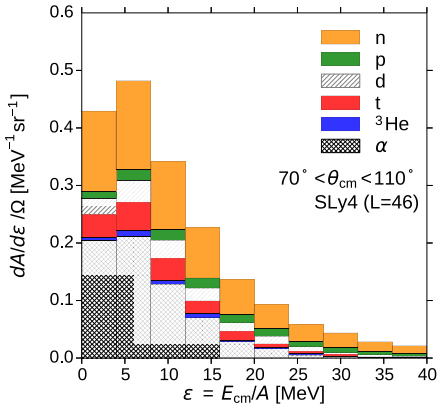

Figure 8. The calculated mass-weighted distributions of the energies $\varepsilon = E/A$ of light particles emitted to the angles $70° < \theta < 110°$ in the center-of-mass system of ^{124}Sn + ^{124}Sn central collisions at 50 MeV/nucleon.

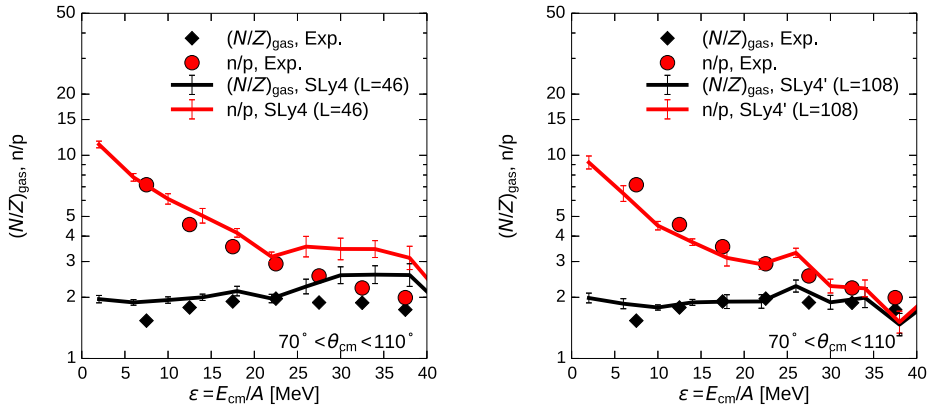

Figure 9. The spectral n/p ratio of free neutrons and protons (red) and the $(N/Z)_{\rm gas}$ ratio for the sum of light particles (black). The lines show the calculated results by AMD with cluster correlations. The adopted effective interaction for the left panel is the Skyrme SLy4 interaction corresponding to a relatively soft symmetry energy $L = 46$ MeV, and that for the right panel is a modified version of SLy4 which corresponds to a stiffer symmetry energy $L = 108$ MeV. The experimental data from Ref. [26] are shown by points.

4 Clusters and the symmetry energy effects

4.1 Neutron-proton ratio at 50 MeV/nucleon

We choose here a typical system of central ^{124}Sn+^{124}Sn collisions at 50 MeV/nucleon. Such a neutron-rich system is suitable to see the effect of the density dependence of the symmetry energy $S(\rho)$ or the parameter $L = 3\rho_0(dS/d\rho)_{\rho_0}$. In the early stage of collisions, the difference of the calculated neutron and proton densities in the high density region shows a very clear effect of the density dependence of the symmetry energy. In the late stage of the reaction, the calculation clearly shows that the symmetry energy influences the degree of fractionation, i.e., how much the gas part is neutron rich compared with the liquid part of the system. Fragment nuclei with $Z \gtrsim 3$ are usually regarded as belonging to the liquid part, while the gas part consists of emitted nucleons and light clusters. The effects in

some final observables studied with a version of AMD were shown in Ref. [25]. Direct information of the liquid part may be obtained from the isotope distribution of fragment nuclei. The width of the isotope distribution has been found to be sensitive to the symmetry energy parameter L, as well as the mean value of the distribution. However, in order to obtain a robust constraint on the L parameter from the comparison with experimental data, it is necessary to better understand the decay of primary fragments. On the other hand, direct information of the gas part should be observed in the yields and spectra of nucleons and light clusters (see Ref. [26] and references therein). It is evidently important to have a good theoretical understanding of emission of clusters.

In order to better understand the composition of the gas part, Fig. 8 shows the distributions of the kinetic energy per nucleon $\varepsilon = E_{\rm cm}/A$ for the nucleons and clusters emitted in transverse directions $70^\circ < \theta_{\rm cm} < 110^\circ$. Each colored area shows the number of the specific cluster multiplied by the cluster mass number A, so that the figure shows the decomposition of nucleons into clusters for each ε. Except for the high energy part, the α cluster formation is quite important since about half of gas nucleons are bound in α particles. The neutron-proton ratio is $(N/Z)_{\rm gas} \approx 2$ for the sum of these particles ($A \leq 4$). This is significantly larger than the ratio $(N/Z)_{\rm system} = 1.48$ for the total system, which is understood as the effect of neutron fractionation. Since the same numbers of neutrons and protons are bound in many α particles (and deuterons), only a small number of protons and ^{3}He are left. Consequently the free n/p ratio and the $t/^3$He ratio can be very large, due to the simple relation

$$\frac{N_{\rm gas} - 2n_\alpha}{Z_{\rm gas} - 2n_\alpha} \gg \frac{N_{\rm gas}}{Z_{\rm gas}}, \tag{11}$$

with n_α being the number of α particles. In Fig. 9, the free n/p ratio is compared with the experimental values from Ref. [26]. The n/p ratio can be very large ($\sim$ 10 at low energies) due to the above-mentioned effect of the α-particle formation. The exact value of the n/p ratio is probably quite sensitive to the details of the emission of α particles. On the other hand, the $(N/Z)_{\rm gas}$ ratio for the sum of these light particles takes a moderate value (~ 2) without a strong dependence on the energy ε.

It seems that the present calculation with the Skyrme SLy4 interaction (corresponding to $L = 46$ MeV) is overestimating the n/p and $(N/Z)_{\rm gas}$ ratios compared to the data as shown in the left part of Fig. 9. In order study the effect of the density dependence of the symmetry energy, we also performed calculations with a force obtained by changing the density dependent term in the SLy4 force

$$v_\rho^{(L=46)} = \tfrac{1}{6}t_3(1 + x_3P_\sigma)\rho(\mathbf{r}_1)^\alpha\delta(\mathbf{r}_1 - \mathbf{r}_2) \tag{12}$$

to

$$v_\rho^{(L=108)} = \tfrac{1}{6}t_3(1 + x_3'P_\sigma)\delta(\mathbf{r}_1 - \mathbf{r}_2)\rho(\mathbf{r}_1)^\alpha + \tfrac{1}{6}t_3(x_3 - x_3')\rho_0^\alpha P_\sigma\delta(\mathbf{r}_1 - \mathbf{r}_2). \tag{13}$$

By choosing $x_3' = -0.5$, we have a force corresponding to $L = 108$ MeV with the same equation of state of symmetric nuclear matter and with the same $S(\rho_0)$ as the original SLy4 force. The results with this stiffer symmetry energy ($L = 108$ MeV) are shown in the right part of Fig. 9. A clear effect of the density dependence of the symmetry energy is seen in the n/p and $(N/Z)_{\rm gas}$ ratios by comparing the left and right parts. This effect is consistent with the stronger fractionation for the lower value of L which corresponds to the larger value of the symmetry energy $S(\rho)$ at subsaturation densities $\rho \leq \rho_0$. It might be possible to obtain a constraint on L by the comparison with experimental data. However, one should carefully check the consistency with other observables because these ratios may be quite sensitive to the details of cluster formation.

4.2 Nuetron-proton dynamics at 300 MeV/nucleon

Heavy-ion collisions at several hundred MeV/nucleon provide us an opportunity to explore compressed nuclear matter. In this subsection, we will discuss the impacts of clusters in the dynamics

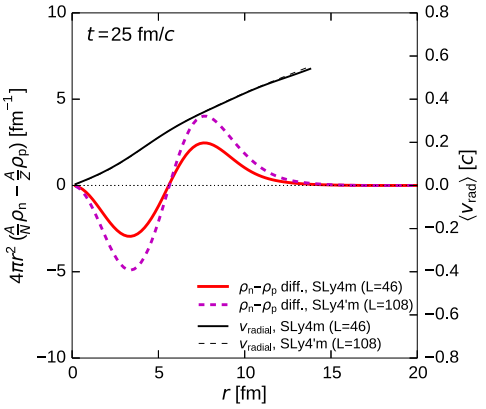

Figure 10. The difference between neutron and protons densities defined as in the text as a function of the distance from the center of the system at the time t = 25 fm/c in ^{132}Sn + ^{124}Sn central collisions at 300 MeV/nucleon. The collective radial velocity is also shown. From Ref. [18].

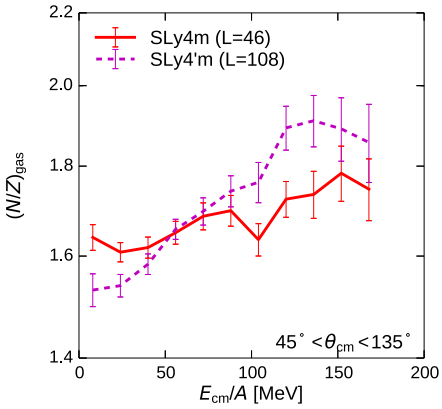

Figure 11. The $(N/Z)_{gas}$ ratio for the sum of emitted particles $1 \le A \le 4$ for the final state of the same reaction system. From Ref. [18].

of ^{132}Sn + ^{124}Sn central collisions at 300 MeV/nucleon by employing the result of the AMD calculation with cluster correlations of Ref. [17]. The details of this calculation are different from Sec. 2. The same discussion for the dynamics of neutrons and protons was given in Ref. [18]. The pion observables are discussed in Ref. [17].

In the AMD calculation with clusters, the maximum density slightly higher than $2\rho_0$ is reached at about t = 20 fm/c, in ^{132}Sn + ^{124}Sn central collisions at 300 MeV/nucleon. In such neutron rich systems, the neutron-proton ratio in the compressed part of the system is sensitive to the value of the symmetry energy at high densities [27]. Figure 10 shows the neutron-proton density difference at t = 25 fm/c defined by

$$\Delta_{np}(r) = 4\pi r^2 \left[\frac{A}{N}\rho_n(r) - \frac{A}{Z}\rho_p(r)\right] \tag{14}$$

for the angle-averaged densities $\rho_n(r)$ and $\rho_p(r)$. The coefficients are defined by using A, N and Z of the reaction system so that we have $\int_0^\infty \Delta_{np}(r)dr = 0$. The results are shown by two lines for the effective interactions corresponding to L = 46 MeV (solid) and L = 108 MeV (dashed). As expected, the central high-density part becomes less neutron rich than the exterior low-density part, and the effect is stronger for the stiffer symmetry energy.

An important question is, of course, how this effect at an early stage can be observed in experiments. The charged pion ratio can be a good probe [17, 27]. We here explore another complementary possibility of using spectra of nucleons and clusters. A hint is found in Fig. 10 in which the radial expansion velocity is also shown. The almost linear dependence on the distance from the center suggests that the system is very simply expanding in this high energy collision. Therefore the exterior part, which is neutron rich, will contribute to the high velocity particles in the final state, while the neutron-poor interior part will be observed as low velocity particles. In fact, this very simple picture seems correct in the calculation as in Fig. 11 which shows the $(N/Z)_{gas}$ spectral ratio for the sum of light particles $1 \le A \le 4$. The relation between the two lines for the different density dependences of the symmetry energy in the $(N/Z)_{gas}$ spectral ratio is similar to $\Delta_{np}(r)$ in Fig. 10.

It should be noted that in the literature the n/p spectral ratio has been found to be insensitive to the density dependence of the symmetry energy, while it is sensitive to the neutron-proton effective mass difference [28], based on the stochastic mean field (SMF) calculation without cluster correlations. On the other hand, the present AMD calculation takes into account the cluster correlations. In fact, when we turn off the cluster correlations in AMD, we find the sensitivity to the symmetry energy is lost in the $(N/Z)_{\rm gas}$ spectral ratio. This suggests that the expansion dynamics is largely influenced by cluster correlations, which is understandable because the number of particles (namely clusters and nucleons) is smaller in the calculation with cluster correlations than without them. The interaction between particles ceases at an earlier time with cluster correlations, while the interaction between nucleons continues longer in the calculations without clusters so that the final neutron and proton spectra are modified from those at early times. This effect is similar to what we found in a different context in the comparison of AMD and SMF [29].

5 Summary

Clusters are important in heavy-ion collisions, not only simply because they are emitted, but also because formation and existence of light clusters influence very much the global reaction dynamics and the bulk nuclear matter properties. AMD has been extended to include cluster correlations in the final states of two-nucleon collisions. The binding of several clusters to form a nucleus should also be considered. The momentum fluctuations of emitted particles also play an important role. The consistent reproduction of basic character of multifragmentation is much more satisfactory than before. This suggests that the excited nuclear many-body systems realized in heavy-ion collisions have stronger cluster correlations than usually expected from single-particle motions in the mean field picture. The fragmentation in a proton induced reaction was also found to be well described when cluster correlations are taken into account. Some observables, such as the n/p spectral ratio, are sensitive to the α-particle formation. If cluster correlation is strong, the expansion is simple in collsions at 300 MeV/nucleon so that the high-density effect of the symmetry energy is reflected almost directly in the $(N/Z)_{\rm gas}$ spectral ratio.

Acknowledgments

This work was supported by JSPS KAKENHI Grant Numbers 21540253 and 24105008. The numerical calculations were partly carried out on SR16000 at YITP in Kyoto University.

References

[1] S. Hudan *et al.*, Phys. Rev. C **67** (2003) 064613.
[2] W. Reisdorf *et al.*, Nucl. Phys. A **848** (2010) 366.
[3] K. Kwiatkowski *et al.*, Phys. Rev. Lett. **50** (1983) 1648.
[4] J. Aichelin, Phys. Rep. **202**, 233 (1991).
[5] A. Ono, H. Horiuchi, T. Maruyama and A. Ohnishi, Prog. Theor. Phys. **87** (1992) 1185.
[6] T. Maruyama, K. Niita, T. Maruyama, and A. Iwamoto, Prog. Theor. Phys. **98** (1997) 97.
[7] T. Maruyama, K. Niita, K. Oyamatsu, T. Maruyama, S. Chiba, and A. Iwamoto, Phys. Rev. C **57** (1998) 655.
[8] A. Ono and H. Horiuchi, Porg. Part. Nucl. Phys. **53**, 501 (2004).
[9] Y. Kanada-En'yo, M. Kimura and A. Ono, Prog. Theor. Exp. Phys. **2012** (2012) 01A202.

[10] A. Ono, J. Phys.: Conf. Ser. **569** (2014) 012086.
[11] G. Röpke, Nucl. Phys. A **867** (2011) 66.
[12] L. Qin *et al.,*, Phys. Rev. Lett. **108** (2012) 172701.
[13] M. Hempel, K. Hagel, J. Natowitz, G. Röpke and S. Typel, Phys. Rev. C **91** (2015) 045805.
[14] P. Danielewicz and G.F. Beartsch, Nucl. Phys. A **533** (1991) 712.
[15] D.D.S. Coupland, W.G. Lynch, M.B. Tsang, P. Danielewicz and Y. Zhang, Phys. Rev. C **84** (2011) 054603.
[16] A. Ono, J. Phys.: Conf. Ser. **420** (2013) 012103.
[17] N. Ikeno, A. Ono, Y. Nara, and A. Ohnishi, in preparation.
[18] A. Ono, a talk given at the 12th International Conference on Nucleus-Nucleus Collisions, June 21–26, Catania, Italy.
[19] A. Ono and H. Horiuchi, Phys. Rev. C **53** (1996) 2958.
[20] Y. Tosaka, A. Ono and H. Horiuchi, Phys. Rev. C **60** (1999) 064613.
[21] A. Ono, S. Hudan, A. Chbihi, J. D. Frankland, Phys. Rev. C **66** (2002) 014603.
[22] A. Ono and H. Horiuchi, Phys. Rev. C **53** (1996) 845.
[23] C. Gale, G. Bertsch, and S. Das Gupta, Phys. Rev. C **35** (1987) 1666.
[24] K. Hagel *et al.*, Phys. Rev. C **50** (1994) 2017.
[25] A. Ono, J. Phys.: Conf. Ser. **436** (2013) 012068.
[26] D.D.S. Coupland *et al.*, arXiv:1006.4546 [nucl-ex] (2014).
[27] B. A. Li, Phys. Rev. Lett. **88** (2002) 192701.
[28] V. Giordano, M. Colonna, M. Di Toro, V. Greco and J. Rizzo, Phys. rev. C **81** (2010) 044611.
[29] M. Colonna, A. Ono and J. Rizzo, Phys. Rev. C **82** (2010) 054613.